Modeling Carbon Black Reinforcement in Rubber Compound

A. van de Walle* C. Tricot* M. Gerspacher†

October 25, 1996

Abstract

One of the advocated reinforcement mechanisms is the formation by the filler of a network interpenetrating the polymer matrix. The deformation and reformation of the filler network allows explanation of low strain dynamic physical properties of the composite. The present model relies on a statistical study of a collection of elementary mechanical systems. This leads to a mathematical approach of the complex modulus $G^* = G' + iG''$. The storage and loss modulus (G' and G'', respectively), are expressed in the form of two integrals capable of modeling their variation with respect to strain.

1 Introduction

Different approaches have been used to model the typical amplitude-dependence of G^* (see figure 1). Gerspacher, Yang and Starita[1] showed that all G'' versus G' plots could be shifted to the same reference curve while Kraus[2] developped a phenomelogical expression for G^*. Many empirical relation between reinforcement and chemical properties have also been found[3].

But these approaches do not focus on the precise mechanism of reinforcement and energy dissipation. Our study of the effect of carbon black used as a filler in elastomers is based on:

- a simple mechanical model representing the elementary interactions between two aggregates;
- a statistical description of the aggregates that models the collective behavior of a group of aggregates.

We will first describe the general simplifications we made in our model before exposing the mechanical model itself. Our statistical description of a collection of elementary mechanical model will then yield a behavior which compares favorably with experimental results.

*École Polytechnique de Montréal, Departement de Mathématiques Appliquées
†Sid Richardson Carbon Co.

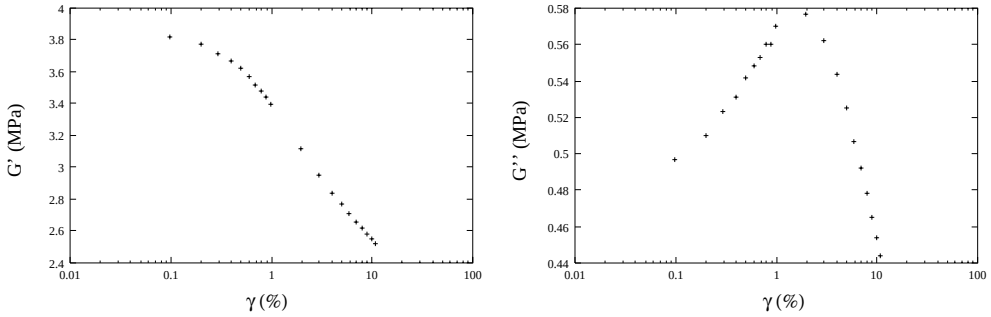

Figure 1: Typical relation between complex modulus and amplitude of deformation

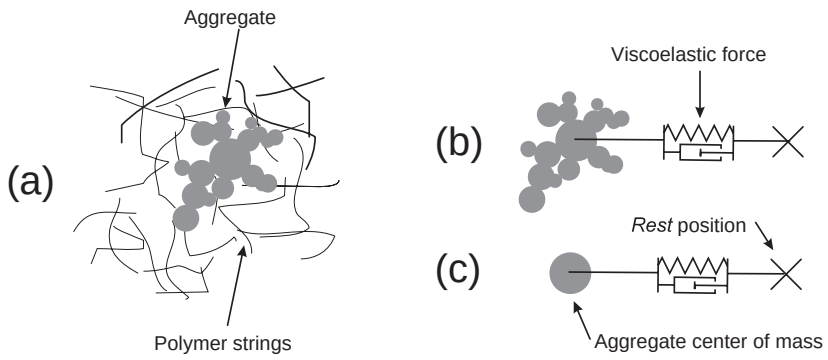

Figure 2: Polymer-aggregate Interaction

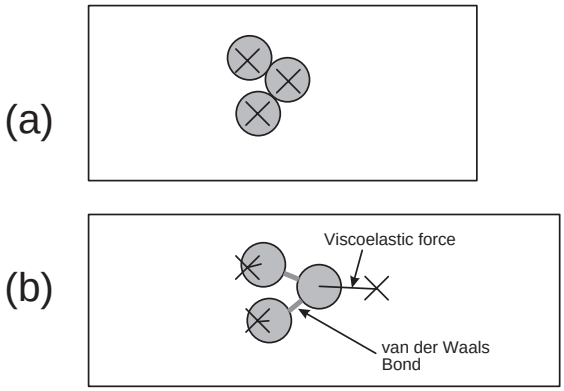

Figure 3: Aggregates (in gray) and equilibrium positions (crosses) under no deformation (a) and when the polymer is stretched (b).

2 Theorical Model

2.1 General Hypotheses of the Model

The complex modulus is assumed to be the sum of two contributions:

- the perfectly linear viscoelastic behavior of the polymer;
- the effect of carbon black aggregates.

We will focus on the second contribution, the first being well-known.

The way carbon black aggregates are embedded in a polymer matrix can be represented by figure 2.1 (a). The polymer strings being much smaller that the aggregates, the polymer matrix can be considered as a viscoelastic continuum. This continuum forces the aggregates to adopt a *rest* positions. Since the polymer is a linear medium, the sum of all strain exerted on an aggregate can be represented by a linear spring-damper system (b) linking the aggregate to its *rest* position (represented by a cross). Considering only the position of the center of mass of the aggregates with respect to its rest position, the system reduces to (c).

The material is composed of many of these aggregates, all of which can be represented by the same simple mechanical model. But when numerous aggregates are brought nearby, another force acts on the aggregates: the London-van der Waals interaction due to neighbouring aggregates.

The effect of stretching the polymer is equivalent to moving the rest positions farther from each other. To evaluate these *new rest* positions, we can interpolate linearly, as shown in figure 2.1 (a) and (b). Notice that because there is a force acting between them, the aggregates do not necessarily remains in their *new rest* positions when the polymer is streched.

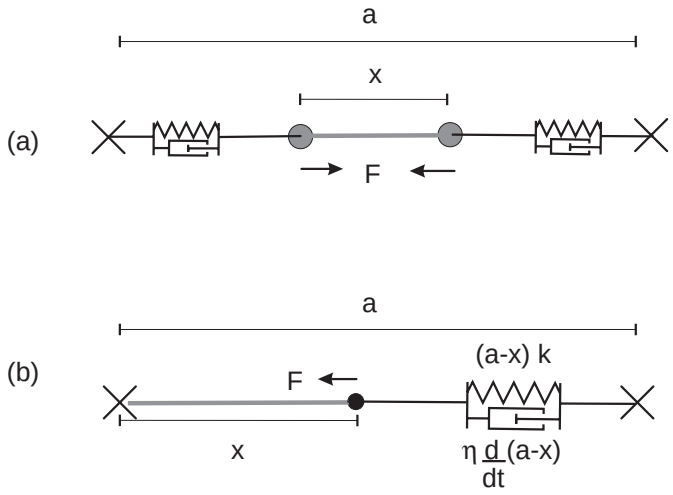

Figure 4: Microscopic mechanical model. k is the elastic constant, η the viscous constant and F the force between the two aggregates.

2.2 Microscopic Interaction Between Aggregates

In this section we will derive an expression that describes the forces which act on the aggregates. But first we need to make some more simplifying assumptions.

The London-van der Waals interaction binding the aggregates is theoretically of infinite range but since its magnitude decreases as the seventh power of the distance, its effect rapidly vanishes. This enables us to focus only on the interactions between almost touching aggregates.

We also assume that the interaction between two aggregates does not influence the behavior of any other pair of aggregates. The problem can thus be considered a sum of N two-body problems instead of a $2N$-body problem. The independence of each two-body problem eases their statistical analysis without introducing too many artefacts, as we will see later on.

The microscopic mechanical model of the interaction between two aggrgates then reduces to figure 2.2 (a). Two spring-damper systems placed in serie can be replaced one equivalent spring-damper system (b). Only remains a string of a spring-damper system (representing the polymer-aggregate interaction) and a non-linear elastic spring (representing the London-van der Waals force).

To model the interaction between the two aggregates, we can use the expression of the London-van der Waals force which has both an attractive term due to the van der Waals force, and a repulsive term accounting for the repulsion between electrons. The exact expression $F(x)$ of this force is however dependent on the exact shape of the aggregates. This shape greatly varies, but in any cases, there is always a region where the force increases (for small distances) and an region where the force decreases (for large distances), as shown in figure 2.2. These descriptive properties are sufficient for our qualitative model.

By inspection of figure 2.2 (b) one can find the equations of movement for x, the aggregate position as a function of time. Since

$$F_{\text{elastic}} + F_{\text{viscous}} - F_{\text{London-van der Waals}} = m\frac{d^2x}{dt^2}$$

where m is the aggregate mass, then

$$(a-x)k + \eta\frac{d}{dt}(a-x) - F(x) = m\frac{d^2x}{dt^2}$$

where η is the viscous constant, k, the spring constant, and a, the distance between the rest positions.

We now seek to plot the curve of F versus a. Suppose that the variation of a is sufficiently slow so that the system has always the time to reach a stationnary state (*i.e.* the process is quasi-static). One must recall that the viscoelastic properties we want to model persist at frequencies as low as 1 hertz. During such slow movement, the composite must have plenty of time to reach equilibrium.

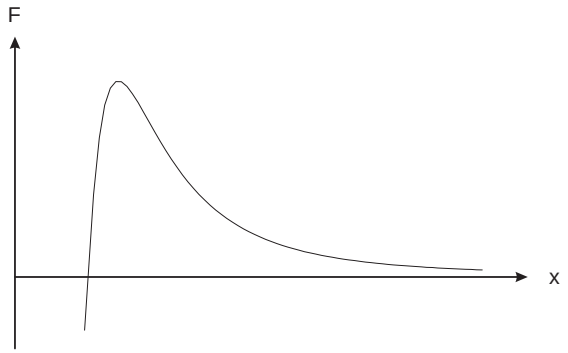

Figure 5: The typical shape of the force F between aggregates as a function of distance x.

Under the quasi-static assumption, both the $\eta\frac{d}{dt}(a-x)$ and the $m\frac{d^2x}{dt^2}$ terms are negligibly small compared to $(a-x)k - F(x)$. So the equation simply reduces to the conditions of static equilibrium:

$$(a-x)k = F(x)$$

This equation can be solved graphically by finding the value F at which the curves $F(x)$ and $(a-x)k$ intersect, for each value of a. Figure 2.2 shows different possible points of intersection.

(a) When no strain is applied on the polymer, $a = a_o$ and the equilibrium position x lies in the increasing region of F $(x = a_0)$.

(b) When a is brought up to a critical value a_b, a second stable equilibrium point appears while the first one disappears. Since there is a rapid jump from one point to another, the London-van der Waals link between the aggregates is said to "break".

(c) For large values of a, the equilibrium point lies in the decreasing region of F.

(d) When a decreases down to a critical value $a_b - \Delta a$, another jump from one equilibrium to a new one occurs. The London-van der Waals link between the aggregates "reforms".

(e) At low values of a, the equilibrium position again lies in the increasing region of F.

Figure 2.2 shows the complete curve that can be obtained by this method. The particular values of a used in figure 2.2 are marked by heavy dots.

Notice the appearance of a hysteresis cycle whose surface gives the energy loss. One may wonder where is the physical origin of the energy loss since the viscous term has been neglected in our derivation. During the fast transition between two equilibrium points, the quasi-static assumption does no longer hold: the viscous force due to the viscoelastic continuum becomes significant and creates great energy losses while the aggregate converges toward the new equilibrium. Despite of that, the quasi-static assumption is a good approximation because:

- the transition is fast and the quasi-static assumption is violated during an infinitesimal amount of time;
- the viscous force also prevents the aggregate from oscillating around its new equilibrium position;
- since energy is conserved, the energy dissipation due to the viscous force (during the fast transitions) must equal the area of the hysteresis cycle.

The viscous term is implicitly taken into account by the appearance of a hysteresis cycle.

One might also be concerned by a third equilibrium point (see figure 2.2 (f)) that we neglected. This point is unstable, as it can be shown from the slope of each curve at the point of intersection.

Let us notice that the exact expression of $F(x)$ is not important. For the qualitative behavior of our model to be correct, the only requirements are that $F(x)$ has:

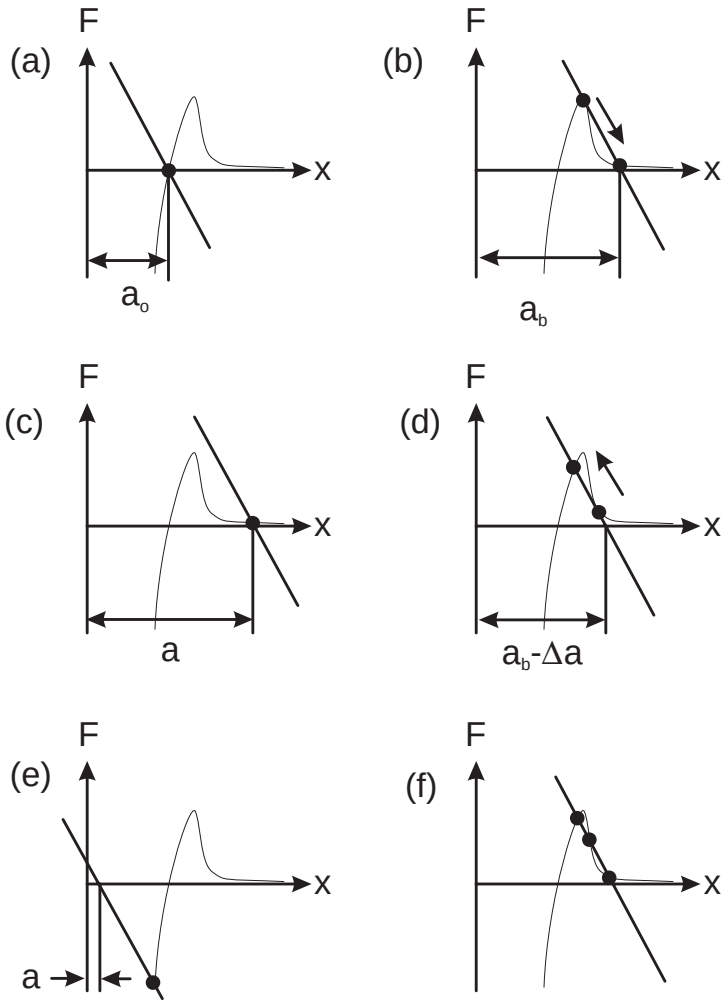

Figure 6: Graphical determination of F versus a.

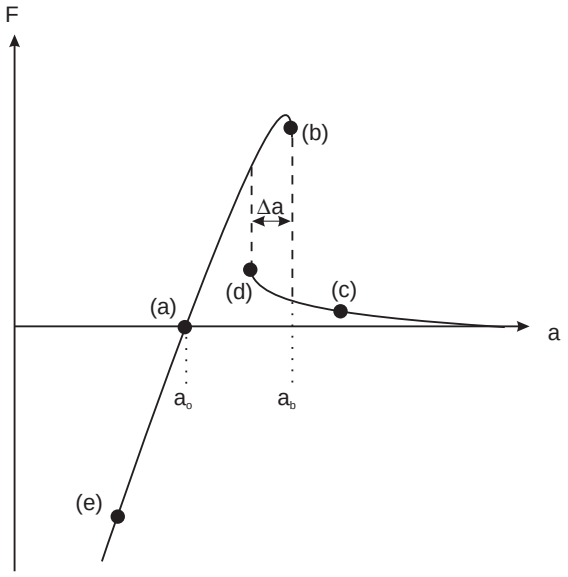

Figure 7: Hysteresis curve of F versus a.

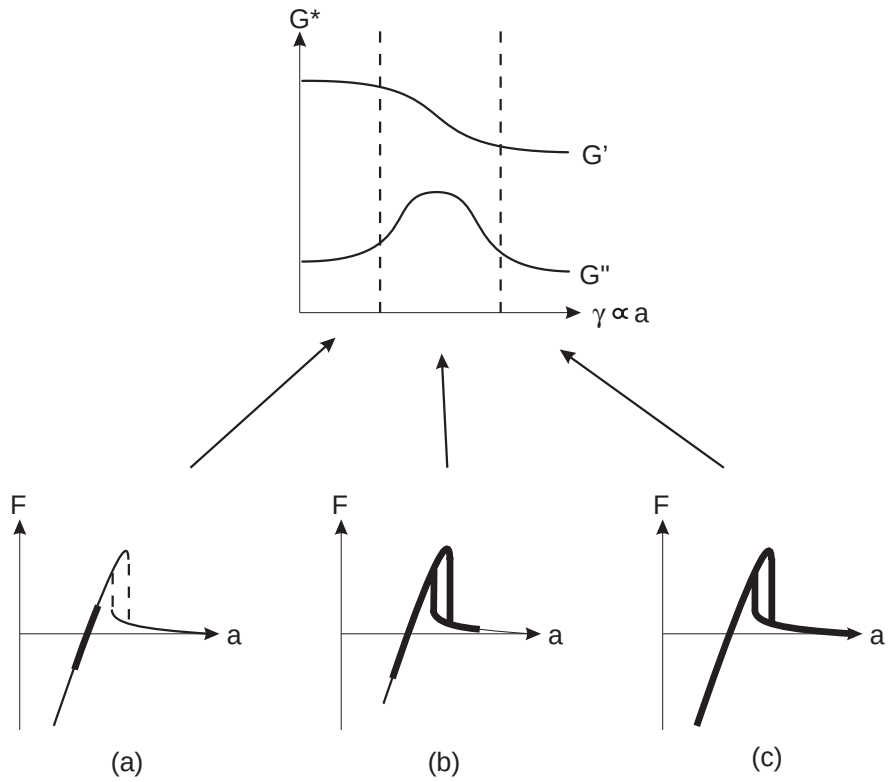

Figure 8: Explanation of the amplitude dependence of G' and G''.

- an increasing and a decreasing region;
- an interval where $-\frac{dF(x)}{dx} > -k$.

Let us now consider qualitatively what happens at different amplitudes of sinusoidal deformation (see figure 2.2).

- At low amplitudes, the deformation is insufficient for the system to reach the critical point where hysteresis appears (2.2a). Energy losses are low and so G'' is small. G' is large since the slope of F is steep.
- At moderate amplitudes (2.2b), the hysteresis appears, and increased energy loss causes G'' to increase. Since the average slope of F decreases, G' also decreases.
- At high amplitudes (2.2c), the losses do not increase much, because they are mainly produced by the hysteresis cycle, which keeps the same area. But since

  $$(\text{Energy losses}) \propto G''(\text{Amplitude})^2$$

  an increased amplitude at constant energy loss yields a decrease of G''.

Until now, we have only considered the behavior of a pair of aggregates and qualitatively described how this behavior influences the values of G' and G'' at different amplitudes. It the next section, we will derive an expression of the contribution of a pair of aggregates to the complex modulus.

2.3 Idealized Response of the Microscopic Model

In order to make our statistical description more manageable mathematically, we must first construct an idealized version of the mechanical model. Under a small deformation, the distance a between rest positions

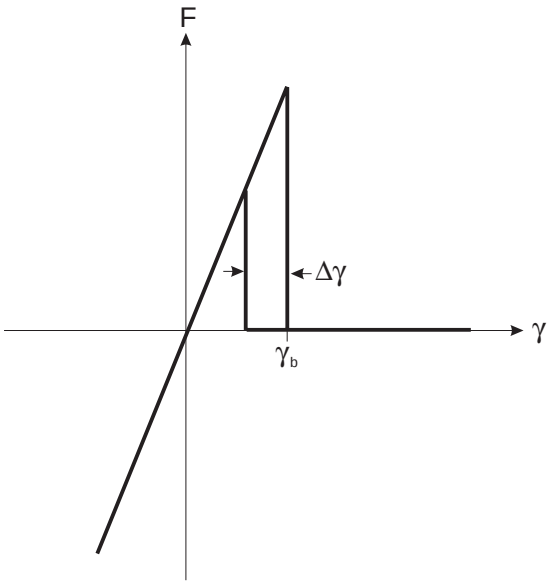

Figure 9: Idealized Response as a function of γ

is assumed to be linearly related to the shear strain γ:

$$a = a_o(1 + r\gamma)$$

which becomes, under a sinusoidal deformation,

$$a = a_o(1 + r\gamma_o \sin\omega t)$$

where r is parameter depending on the spatial orientation of a given aggregate pair. The plot of F versus γ is thus similar to figure 2.2. If we also linearize each curved portion of the curve, we obtain figure 2.3. Here follows a derivation of the complex viscoelastic constant $g^* = g' + ig''$ of this idealized elementary mechanical model.

If F were linear, we would have

$$F = g^*\gamma$$

but we just saw that F is not linear so only an *effective* value of g^* can be found. This *effective* value is defined as the first term of the Fourier series of F as a function of time, when $\gamma = \gamma_0 e^{i\omega t}$. We will use an alternative approach giving an estimate of g^* without relying to Fourier series.

Let us first consider the imaginary part of g^* which is directly related to energy loss (E_l). When $\gamma_o < \gamma_b$, there is no energy loss since the hysteresis does not take place. At the onset of the hysteresis cycle at $\gamma_o = \gamma_b$ E_l equals the area enclosed by the hysteresis cycle, which can be approximated by

$$E_l \approx g_0\,\gamma_b\,\Delta\gamma$$

where g_0 is the slope of the increasing region of F versus γ and $\Delta\gamma$ is the width of the hysteresis cycle. (see figure 2.3 (a)).

Recalling that

$$G'' \propto \frac{E_l}{\gamma_o^2}$$

we find, analogously:

$$g''(\gamma_o, \gamma_b) = \begin{cases} 0 & \text{if } \gamma_o \le \gamma_b \\ \frac{E_l}{\gamma_o^2} & \text{if } \gamma_o > \gamma_b \end{cases}$$

Figure 2.3 (b) shows g'' as a function of γ_o.

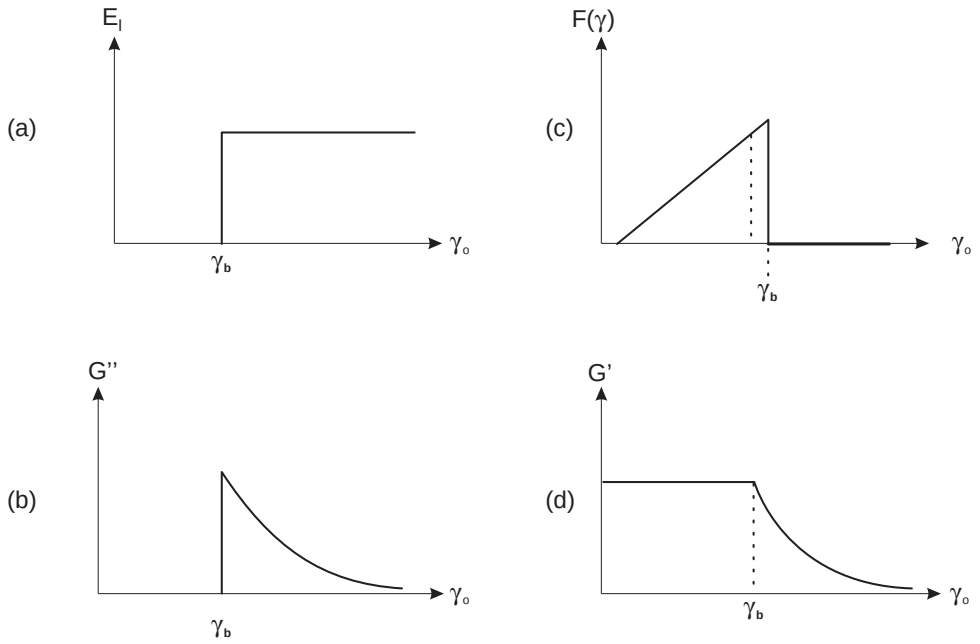

Figure 10: Idealized microscopic viscoelastic constants

An estimate of the effective g' is obtained by computing a linear regression of F versus γ on the interval $[0, \gamma_o]$. (A more rigorous treatment would require to consider the interval $[-\gamma_o, \gamma_o]$ instead. But it would only adds a constant amplitude-independant contribution to g'.) If we assume that the width of the hysteresis cycle is small, the curve F versus γ reduces to the graph $F(\gamma)$ shown in figure 2.3 (c). For $\gamma_o \leq \gamma_b$, the regression yields a slope of g_0 while for $\gamma_o > \gamma_b$ the slope is given by:

$$g'(\gamma_o, \gamma_b) \approx \frac{\int_0^{\gamma_o} \gamma F(\gamma) d\gamma}{\int_0^{\gamma_o} \gamma^2 d\gamma} = \frac{\int_0^{\gamma_b} \gamma F(\gamma) d\gamma}{\frac{\gamma_o^3}{3}} = \frac{\int_0^{\gamma_b} g_0 \gamma^2 d\gamma}{\frac{\gamma_o^3}{3}} = \frac{g_0 \gamma_b^3}{\gamma_o^3}$$

In summary, the idealized description of the microscopic viscoelastic (g^*) constant as a function of γ_o, is:

$$g^*(\gamma_o, \gamma_b) = g_0 s'(\gamma_o, \gamma_b) + i g_0 \left(\frac{\Delta\gamma}{\gamma_b} \right) s''(\gamma_o, \gamma_b)$$

where

$$s'(\gamma_o, \gamma_b) = \left\{ \begin{array}{ll} 1 & \text{if } \gamma_o \leq \gamma_b \\ \frac{\gamma_b^3}{\gamma_o^3} & \text{if } \gamma_o > \gamma_b \end{array} \right\} \quad \text{and} \quad s''(\gamma_o, \gamma_b) = \left\{ \begin{array}{ll} 0 & \text{if } \gamma_o \leq \gamma_b \\ \frac{\gamma_b^2}{\gamma_o^2} & \text{if } \gamma_o > \gamma_b \end{array} \right\}$$

Figure 2.3 (b) et (d) show the real and imaginary part of $g^*(\gamma_o, \gamma_b)$.

2.4 Statistical Description

It seems that the idealized response derived in the last section yields a behavior too discontinuous to compare favorably with experimental results. But one must recall that the composite is made of many pairs of aggregate, each of which breaks and reforms at different times in the cycle. The resulting macroscopic response $G^*(\gamma)$ is then a smoothed version of $g^*(\gamma, \gamma_b)$ as shown in figure 2.4.

We identified two major causes of smoothing:

- During uniaxial or shear deformation, the relative displacement of the pairs of aggregates is dependent on the orientation of the pair. So a given macroscopic deformation produces a range of values of microscopic deformation.

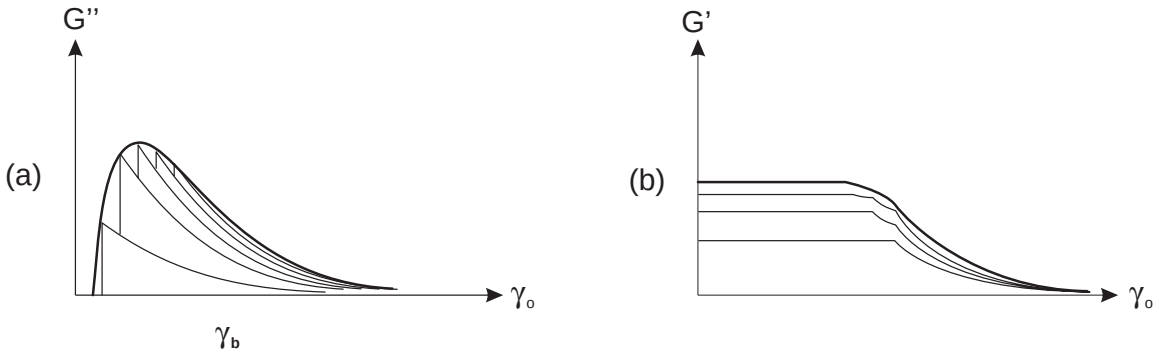

Figure 11: The smoothing effect of distributed values of γ_b

- The binding energy of the van der Waals links is not constant: for a given microscopic deformation, some pairs break, other do not.

These two effects give rise to two distributions that are convoluted together to yield a single distribution function. Let $N(\gamma_b)d\gamma_b$ be that function which gives the number of links that break when the polymer is stretched from γ_b to $\gamma_b + d\gamma_b$. The complex complex modulus is then given by:

$$G^*(\gamma) = \int_0^\infty g_0(\gamma_b)s'(\gamma,\gamma_b)N(\gamma_b)d\gamma_b + i\int_0^\infty g_0(\gamma_b)hs''(\gamma,\gamma_b)N(\gamma_b)d\gamma_b$$

where h is the average value of $\frac{\Delta\gamma}{\gamma_b}$. By taking the average value of the ratio $\frac{\Delta\gamma}{\gamma_b}$ we assume that h follows a distribution which is independent of γ_b. Under the same assuption, we can factor h out of the integral.

Note that the effect of $g_0(\gamma_b)$ is undistiguishable from the one of $N(\gamma_b)$ because the effect of a great number of weak links is undistinguishable from the one of a small number of strong links. We then combine $g_0(\gamma_b)$ and $N(\gamma_b)$ into one weighting function:

$$W(\gamma_b) = g_0(\gamma_b)N(\gamma_b)$$

The system then reduces to:

$$G^*(\gamma) = \int_0^\infty s'(\gamma,\gamma_b)W(\gamma_b)d\gamma_b + ih\int_0^\infty s''(\gamma,\gamma_b)W(\gamma_b)d\gamma_b$$

This equation complety describes the system. The exact forms of $s'(\gamma,\gamma_b)$ and $s''(\gamma,\gamma_b)$ are known but

- the constant h and
- the function $W(\gamma_b)$

have yet to be determined from experimental data.

$G'(\gamma)$ and $G''(\gamma)$ are expressed as the convolution of the same weighting function $W(\gamma_b)$ with known functions $s'(\gamma,\gamma_b)$ and $s''(\gamma,\gamma_b)$. This helps to explain why there is a very similar relation between G' and G'' for different carbon black composites. The functions $s'(\gamma,\gamma_b)$ and $s''(\gamma,\gamma_b)$ remain the same for any material having the kind of dissipation mecanism we described here. On the other hand, $W(\gamma_b)$ is dependent on the precise type of composite.

We can now see why the two-body assumption introduced in section 2.2 does not alters the validity of our model. It is true that the breakage of one van der Waals link may change the force acting between other pairs of aggregates. However, this will only change the value γ_b at which other pairs will break: functions $s'(\gamma,\gamma_b)$ and $s''(\gamma,\gamma_b)$ remain unaffected while the distribution $W(\gamma_b)$ can be adjusted to take this possibility into account.

3 Experimental Results

What can be done now to test this model? After all, the unknown function $W(\gamma_b)$ gives us an infinite number of degrees of freedom. It is indeed easy to find a $W(\gamma_b)$ such that $G''(\gamma)$ fits experimental data. But then, for the same $W(\gamma_b)$, $G'(\gamma)$ has to fit also. The criterion that $G'(\gamma)$ and $G''(\gamma)$ must both fit gives us the ultimate test of our model. Figures 4 through 4 show that this is actually the case.

To obtain these figures, we use the graph of $G''(\gamma)$ to find the function $W(\gamma_b)$. If we express our integrals as a finite sums, the process reduces to the simple problem of solving a finite system of linear equations. We then compute $G'(\gamma)$ from $W(\gamma_b)$, again using discrete integrals. The value of h is finally ajusted to give the best fit.

For that procedure to work, one must first substract the constant contribution of the polymer (noted $G_p^* = G_p' + iG_p''$) from the values of G' and G''. The horizontal lines on the graphs of G' and G'' show the values used in the computations.

Note that the the constant contribution G_p^* is not equal to the complex modulus of the pure polymer, because carbon black also behaves as a rigid and inert filler which adds a constant contribution to G^*. In fact, G_p^* is the complex modulus of the polymer mixed with with a filler identical to carbon black but having no van der Waals bondings.

4 Conclusion

Here are the most important steps of the derivation of our model:

- Two phenomena contribute to the complex modulus: the linear viscoelastic behavior of the polymer matrix, and the non-linear elastic behavior of carbon black.
- Upon deformation, the polymer pulls the aggregate appart while the London-van der Waals force pushes them together.
- Because of the particular shape of the London-van der Waals force, two stable equilibrium points are possible for a pair of aggregate: they can be "bound" or "unbound".
- The transition from the bound to unbound state is the cause of G' decrease when γ increases.
- The high speed at which the transistion from bounded to unbouded state occurs produces increased energy loss via increased friction in the polymeric continuum due to a high deformation rate. This is the cause of the peak in the plot of G'' versus γ.
- An expression of the viscoelastic constant of the idealized model of a pair of aggregates can be found. Its real and imaginary parts, respectively, are proportionnal to:

$$s'(\gamma,\gamma_b) = \begin{cases} 1 & \text{if } \gamma \le \gamma_b \\ \frac{\gamma_b^3}{\gamma^3} & \text{if } \gamma > \gamma_b \end{cases}$$

$$s''(\gamma,\gamma_b) = \begin{cases} 0 & \text{if } \gamma \le \gamma_b \\ \frac{\gamma_b^2}{\gamma^2} & \text{if } \gamma > \gamma_b \end{cases}$$

  where

  - γ is the ampitude of sinusoidal shear deformation;
  - γ_b is the amount of deformation causing the pair to unbind.

- The composite is made of a collection of those elementary models, each having a different γ_b. We then express the complex modulus of the material as:

$$G^*(\gamma) = \int_0^\infty s'(\gamma,\gamma_b)W(\gamma_b)d\gamma_b + ih\int_0^\infty s''(\gamma,\gamma_b)W(\gamma_b)d\gamma_b$$

  where

  - $W(\gamma_b)$ is a weighting function giving the contribution of aggregate pairs which break at $\gamma = \gamma_b$ and
  - h is a constant proportionnal to the average width $\Delta\gamma$ of the hysteresis cycle.

- With this expression, one can see why plots of G'' versus G' for different polymers are so similar. The expression of s' and s'' are universal, while $W(\gamma_b)$ is material-dependent. There is a link between G' and G'' because they are derived from the convolution of the same function $W(\gamma_b)$. The link remains accross different materials because $s'(\gamma, \gamma_b)$ and $s''(\gamma, \gamma_b)$ are material-independent.

- This model can be easily tested by showing that there exists a function $W(\gamma_b)$ such that $G'(\gamma)$ and $G''(\gamma)$ can be both made to fit experimental data.

What still remains to be done is to:

- test the validity of the model over a wider range of experimental results;

- develop a precise expressions for $W(\gamma_b)$.

References

[1] Krauss, G., J. Appl. Polymer Sci., Appl. Polymer Symposium, **39**, 75 (1984).

[2] Gerspacher, M., Yang, H. H., Starita J. M., L'actualité chimique, **106**, March-April (1991).

[3] Wolff S. and Wang M. J. in "Carbon Black", Donnet J.-B., Bansal R. C., Wang, M.-J., Ed., Marcel Dekker, New York, 1993, ch. 9.

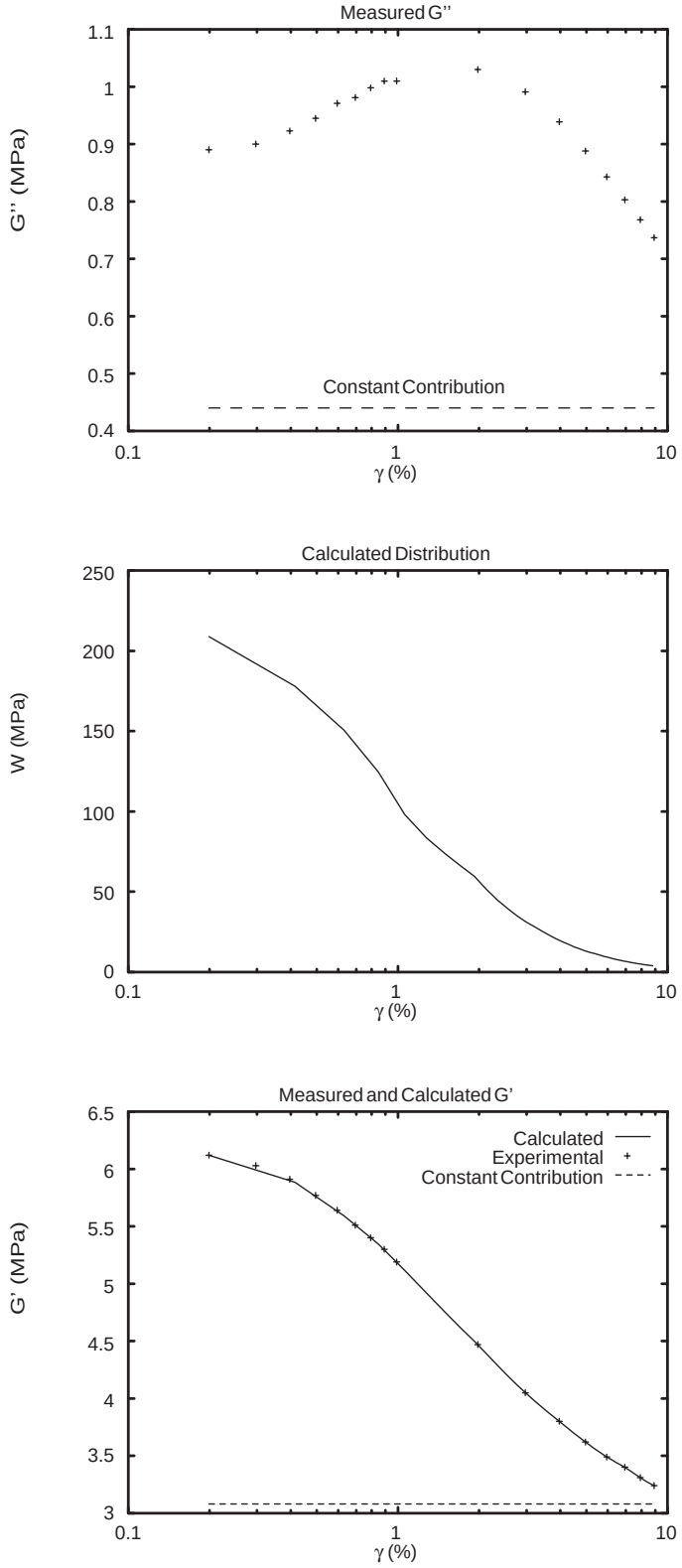

Figure 12: From top to bottom: experimental values of $G''(\gamma)$ for SBR/N110 composite; Computed values of $W(\gamma_b)$ for SBR/N110 composite; Computed and experimental values of $G'(\gamma)$ for SBR/N110 composite.

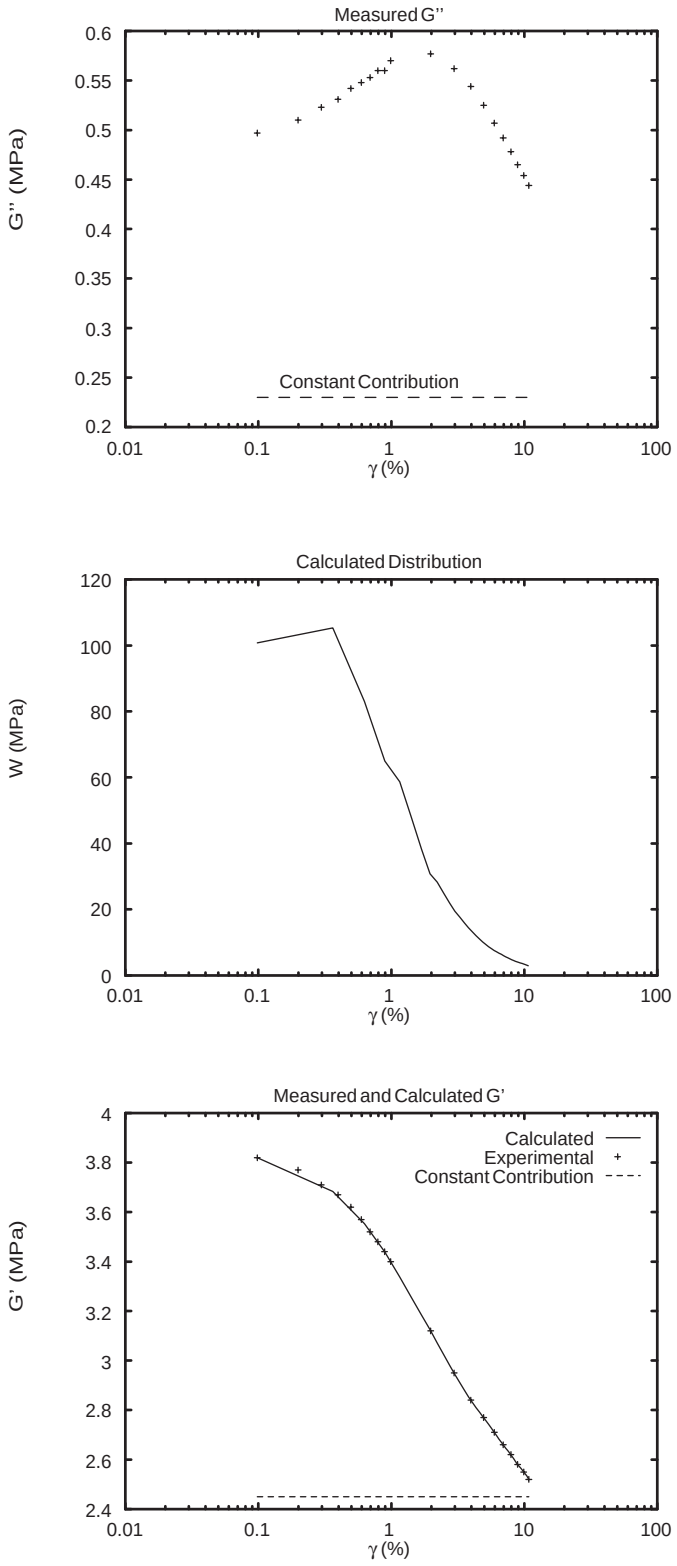

Figure 13: From top to bottom: experimental values of $G''(\gamma)$ for SBR/N330 composite; computed values of $W(\gamma_b)$ for SBR/N330 composite; computed and experimental values of $G'(\gamma)$ for SBR/N330 composite.

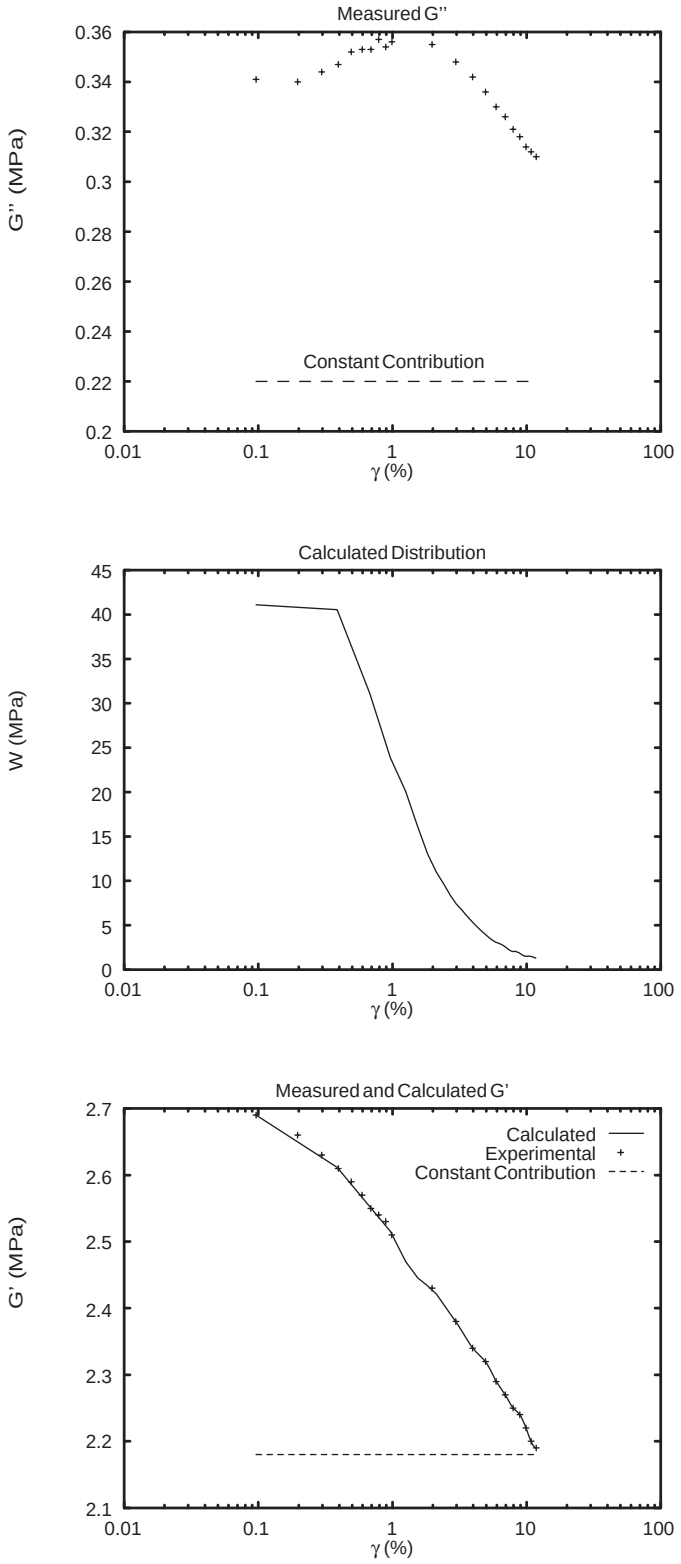

Figure 14: From top to bottom: experimental values of $G''(\gamma)$ for SBR/N550 composite; computed values of $W(\gamma_b)$ for SBR/N550 composite; computed and experimental values of $G'(\gamma)$ for SBR/N550 composite.

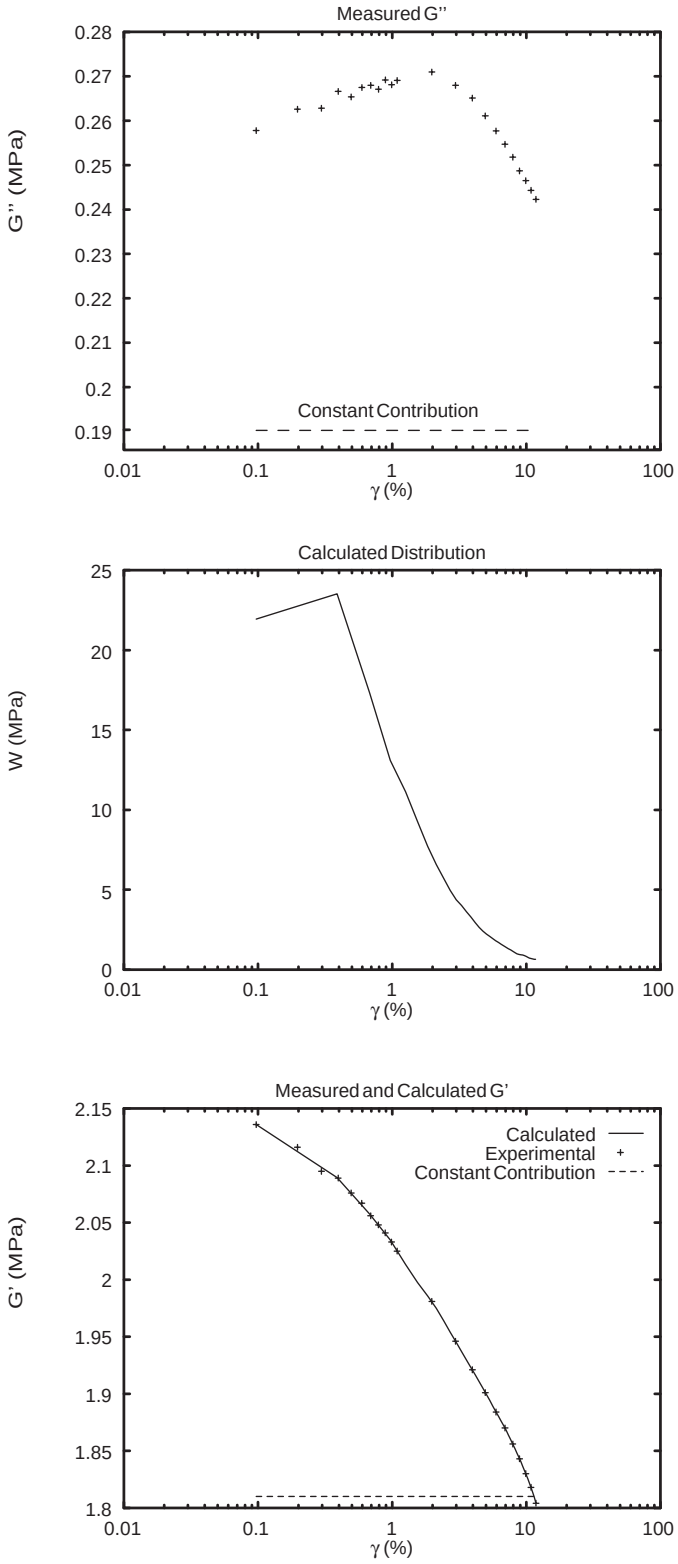

Figure 15: From top to bottom: experimental values of $G''(\gamma)$ for SBR/N762 composite; computed values of $W(\gamma_b)$ for SBR/N762 composite; computed and experimental values of $G'(\gamma)$ for SBR/N762 composite.